

Weak-coupling phase diagram of the two-chain Hubbard model

Leon Balents and Matthew P. A. Fisher

Institute for Theoretical Physics, University of California, Santa Barbara, California 93106-4030

(Received 30 August 1995; revised manuscript received 9 November 1995)

We present a general method for determining the phase diagram of systems of a finite number of one-dimensional Hubbard-like systems coupled by single-particle hopping with weak interactions. The technique is illustrated by detailed calculations for the two-chain Hubbard model, providing controlled results for arbitrary doping and interchain hopping. Of nine possible states which could occur in such a spin-1/2 ladder, we find seven at weak coupling. We discuss the conditions under which the model can be regarded as a one-dimensional analog of a superconductor.

I. INTRODUCTION

One-dimensional (1D) electron systems provide an important testing ground for understanding electron-correlation effects. Many methods have been applied to the problem of a single Hubbard chain, and there is general agreement that the system remains, for repulsive interactions, in a Luttinger-liquid state with gapless spin and charge modes.¹ The 1D analog of a superconductor, a state with one gapless charge mode and dominant pairing (rather than charge-density wave) correlations, does not arise in that case.

Two-chain systems are interesting as a first step towards true 2D materials, and may be relevant for some experimental systems.² Moreover, on a ladder, statistics are more important, since particles can exchange without passing through one another. However, the theoretical situation in such models is much less clear.³⁻⁸ Recent simulations suggest that states with dominant pairing correlations can indeed arise.⁹

In this paper, we present a systematic weak-coupling analysis of two Hubbard chains coupled by single-particle hopping, t_{\perp} . Our approach is a *controlled* renormalization group valid for small U but for *arbitrary* interchain hopping and filling, n .¹⁰ The general methods described here may be applied to *any* system composed of a finite number of Hubbard-like chains with weak short-range four-fermion interactions.

The possible phases of such models can be characterized by the number of charge and spin modes which are gapless at zero momentum. For an N -chain system the number of gapless charge modes can vary from zero to N , and likewise for spin. Remarkably, of the nine possible phases for two chains, seven are realized within the simple Hubbard model at weak coupling, reflecting the proliferation of marginal operators. Denoting a phase with x gapless charge modes and y gapless spin modes as C_xS_y , the small U phase diagram as a function of interchain hopping t_{\perp} and filling n is shown in Fig. 1. Particularly noteworthy is the phase C1S0, present with purely *repulsive* interactions (positive U). This phase has a spin gap and a *single* gapless charge mode, and is thus the 1D analog of either a superconductor (SC) or charge-density wave (CDW). As found by other authors, the pairing of up and down spins in this phase is “*d*-wave-like,” in the sense that the pair wave function has opposite sign in the bonding

and antibonding bands ($k_{\perp}=0,\pi$).^{9,4} A more precise and general definition of this type of pairing is given below in terms of bosonization.

Two alternative physical criteria distinguish the two possibilities for an array of weakly coupled ladders, depending upon the relative strength of the interladder coupling and of quenched impurities. If the impurity interactions dominate, localization must be avoided within each ladder independently. This requires a very slow decay of pairing correlations.¹¹ In particular, if the equal time pairing correlation function $\langle \Delta(x)\Delta^{\dagger}(0) \rangle \sim 1/|x|^{\kappa}$, where $\Delta = c_{1\uparrow}c_{2\downarrow}$, this requires $\kappa < \kappa_c = 1/3$. If interladder couplings are stronger than impurity scattering, two- (or three-) dimensional phase coherence can set in and further stabilize the SC. It must compete, however, with the formation of a CDW (which, due to pinning, is an insulating phase). For $1/2 < \kappa < 2$, the situation is best summarized in Fig. 2, which shows a schematic phase diagram at fixed disorder as a function of interladder pair-hopping (P) and interladder Coulomb interaction (V). The exponent κ determines the *curvature* of the SC-CDW phase boundary in this plane: $V \sim P^{(2-1/\kappa)/(2-\kappa)}$. The traditional requirement¹² of “dominant SC correlations” gives $\kappa_c = 1$ (see below), and corresponds to a straight line on this plot. Note that for $\kappa < 1/2$ and *any* weak (but still larger than the impurity potential) pair hopping, the system is a SC; conversely, for $\kappa > 2$ and

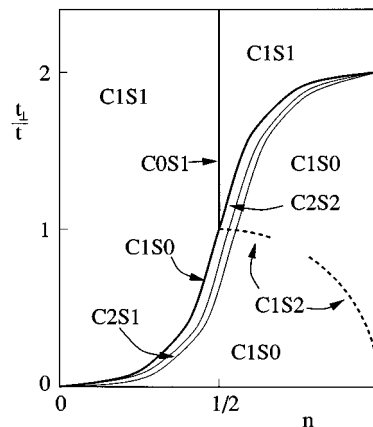


FIG. 1. Phase diagram in the $U \rightarrow 0^+$ limit.

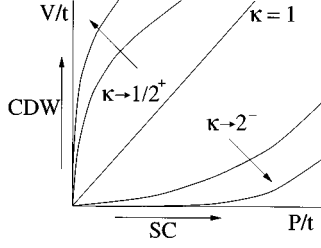


FIG. 2. Fate of the C1S0 phase for various value of κ , provided the interladder pair hopping matrix element is larger than typical impurity pinning energies.

any weak interchain interactions it is a CDW.

Interestingly, the spin-gapped C1S0 phase occurs in two different regimes (Fig. 1), one for doping, $\delta=1-n$, away from half-filling, and the other when the Fermi energy coincides with a band edge, $k_{F1}=0$. In the former case, pairing correlations develop upon doping the spin-gapped Mott insulator at half filling, $n=1$, as in Anderson's original resonating valence bond picture for superconductivity in the cuprates.¹³ The critical doping δ_c at which C1S0 gives way to a gapless spin state, C2S1 and C2S2, is large for weak interchain hopping, decreasing from $\delta_c=1$ for small t_\perp to $\delta_c=0$ as $t_\perp \rightarrow 2t$. Note that the phase C2S2 is the 1D analog of a Fermi liquid with all spin and charge modes gapless. The presence of the spin-gapped state (C1S0) near $k_{F1}=0$, can be attributed to the coincidence of the Fermi energy with the Van Hove singularity at the 1D band edge.

II. MODEL

The two-chain Hubbard model is described by the Hamiltonian $H=H_0+H_U$, with

$$H_0 = \sum_{x,\alpha} \{-t(c_{x,\alpha}^\dagger c_{x+1,\alpha} + c_{\leftrightarrow}) - t_\perp c_{x,\alpha}^\dagger d_{x,\alpha} + \text{H.c.}\},$$

$$H_U = \sum_x U: (c_{x,\uparrow}^\dagger c_{x,\uparrow} c_{x,\downarrow}^\dagger c_{x,\downarrow} + c_{\leftrightarrow}):, \quad (2.1)$$

where c (c^\dagger) and d (d^\dagger) are fermion annihilation (creation) operators on the first and second chain, respectively, and $\alpha = \uparrow, \downarrow$ is a spin index. The parameters t and t_\perp are hopping matrix elements along and between the chains, and U is an on-site Hubbard interaction. Equation (2.1) has the usual $U(1) \times SU(2)$ charge/spin symmetry.

For weak coupling it is natural to proceed by first diagonalizing the quadratic portion of the Hamiltonian. This is achieved by canonically transforming to bonding and antibonding band operators: $\psi_{i\alpha} = (c_\alpha + (-1)^i d_\alpha) / \sqrt{2}$, with $i=1,2$. In momentum space H_0 becomes

$$H_0 = \sum_{i,\alpha} \int_{-\pi}^{\pi} \frac{dp}{2\pi} \epsilon_i(p) \psi_{i\alpha}^\dagger(p) \psi_{i\alpha}(p), \quad (2.2)$$

where $\epsilon_1 = t_\perp - 2t \cos p$ and $\epsilon_2 = -t_\perp - 2t \cos p$. For $t_\perp > 2t$, the two bands are completely separated. At half-filling, the system is then a band insulator, and when doped becomes an ordinary spin-1/2 Luttinger-liquid, denoted

C1S1 (see Fig. 1). For $t_\perp < 2t$, the bands overlap over some range of energies. When the Fermi level lies within this region, interaction effects must be reexamined in detail.

It is sufficient to consider the behavior of the system only near the two Fermi momenta k_{Fi} , defined by $\epsilon_i(k_{Fi}) = \mu$. The chemical potential, μ , is fixed by the requirement $k_{F1} + k_{F2} = n\pi$, where n is the particle number per site. The decomposition $\psi_{i\alpha} \approx \psi_{Ri\alpha} e^{ik_{Fi}x} + \psi_{Li\alpha} e^{-ik_{Fi}x}$ gives, up to a constant

$$H_0 = \sum_{i,\alpha} \int dx v_i (\psi_{Ri\alpha}^\dagger i \partial_x \psi_{Ri\alpha} - \psi_{Li\alpha}^\dagger i \partial_x \psi_{Li\alpha}), \quad (2.3)$$

where $v_i = 2t \sin k_{Fi}$. The allowed four Fermi interactions are highly constrained by symmetry. In addition to $U(2)$ invariance, these terms must be preserved by time reversal, parity, chain interchange, and spatial translation operations. At generic fillings, the two Fermi momenta are incommensurate, and the symmetry under translations is effectively doubled into independent transformations in each band. To delineate the couplings in a physical way, we employ the notation of current algebra,

$$J_{iR} = \psi_{Ri\alpha}^\dagger \psi_{Ri\alpha}, \quad \mathbf{J}_{iR} = \frac{1}{2} \psi_{Ri\alpha}^\dagger \boldsymbol{\sigma}_{\alpha\beta} \psi_{Ri\beta},$$

$$L_R = \psi_{R1\alpha}^\dagger \psi_{R2\alpha}, \quad \mathbf{L}_R = \frac{1}{2} \psi_{R1\alpha}^\dagger \boldsymbol{\sigma}_{\alpha\beta} \psi_{R2\beta},$$

$$M_{iR} = -i \psi_{Ri\uparrow} \psi_{Ri\downarrow}, \quad N_{R\alpha\beta} = \psi_{R1\alpha} \psi_{R2\beta}, \quad (2.4)$$

where $\boldsymbol{\sigma}$ denotes Pauli matrices. Although we have not explicitly indicated it here, all the currents in Eq. (2.4) are defined as normal-ordered quantities (see Appendix A). Left-moving currents are defined analogously. There are eight allowed interactions connecting left and right movers for generic fillings, with Hamiltonian densities

$$-\mathcal{H}_{\text{int}}^{(1)} = \tilde{g}_{1\rho} J_{1R} J_{1L} + \tilde{g}_{2\rho} J_{2R} J_{2L} + \tilde{g}_{x\rho} (J_{1R} J_{2L} + J_{2R} J_{1L})$$

$$+ \tilde{g}_{1\sigma} \mathbf{J}_{1R} \cdot \mathbf{J}_{1L} + \tilde{g}_{2\sigma} \mathbf{J}_{2R} \cdot \mathbf{J}_{2L} + \tilde{g}_{x\sigma} (\mathbf{J}_{1R} \cdot \mathbf{J}_{2L}$$

$$+ \mathbf{J}_{2R} \cdot \mathbf{J}_{1L}) + \tilde{g}_{i\rho} (L_R L_L + L_R^\dagger L_L^\dagger)$$

$$+ \tilde{g}_{i\sigma} (\mathbf{L}_R \cdot \mathbf{L}_L + \mathbf{L}_R^\dagger \cdot \mathbf{L}_L^\dagger). \quad (2.5)$$

Six additional interactions are completely chiral,

TABLE I. Hubbard model coupling constants. The g -ology notation is given for comparison with Ref. 14.

Coupling	g -ology	Hubbard value
$\tilde{g}_{1\rho}$	$g_{AAAA}^1/2 - g_{AAAA}^2$	$-U/4$
$\tilde{g}_{2\rho}$	$g_{BBBB}^1/2 - g_{BBBB}^2$	$-U/4$
$\tilde{g}_{x\rho}$	$g_{ABAB}^1/2 - g_{ABBA}^2$	$-U/4$
$\tilde{g}_{i\rho}$	$g_{AABB}^1/2 - g_{AABB}^2$	$-U/4$
$\tilde{g}_{1\sigma}$	$2g_{AAAA}^1$	U
$\tilde{g}_{2\sigma}$	$2g_{BBBB}^1$	U
$\tilde{g}_{x\sigma}$	$2g_{ABAB}^1$	U
$\tilde{g}_{i\sigma}$	$2g_{AABB}^1$	U

$$\begin{aligned}
-\mathcal{H}_{\text{int}}^{(2)} = & \tilde{\lambda}_{1\rho}(J_{1R}^2 + J_{1L}^2) + \tilde{\lambda}_{2\rho}(J_{2R}^2 + J_{2L}^2) + \tilde{\lambda}_{x\rho}(J_{1R}J_{2R} \\
& + J_{1L}J_{2L}) + \tilde{\lambda}_{1\sigma}(\mathbf{J}_{1R} \cdot \mathbf{J}_{1R} + \mathbf{J}_{1L} \cdot \mathbf{J}_{1L}) + \tilde{\lambda}_{2\sigma}(\mathbf{J}_{2R} \cdot \mathbf{J}_{2R} \\
& + \mathbf{J}_{2L} \cdot \mathbf{J}_{2L}) + \tilde{\lambda}_{x\sigma}(\mathbf{J}_{1R} \cdot \mathbf{J}_{2R} + \mathbf{J}_{1L} \cdot \mathbf{J}_{2L}). \quad (2.6)
\end{aligned}$$

$$\begin{aligned}
-\mathcal{H}_{\text{int}}^{(3)} = & \tilde{g}_{1u}(M_{1R}^\dagger M_{1L} + M_{1L}^\dagger M_{1R}) + \tilde{g}_{2u}(M_{2R}^\dagger M_{2L} + M_{2L}^\dagger M_{2R}) + \tilde{g}_{xu}(M_{1R}^\dagger M_{2L} + M_{1R} M_{2L}^\dagger + M_{2R}^\dagger M_{1L} + M_{2R} M_{1L}^\dagger) \\
& + \tilde{g}_{tu1}(N_{R\alpha\beta}^\dagger N_{L\alpha\beta} + N_{R\alpha\beta} N_{L\alpha\beta}^\dagger) + \tilde{g}_{tu2}(N_{R\alpha\beta}^\dagger N_{L\beta\alpha} + N_{R\alpha\beta} N_{L\beta\alpha}^\dagger). \quad (2.7)
\end{aligned}$$

The single-band umklapp term, \tilde{g}_{iu} , is nonzero only if $k_{Fi} = \pi/2$. At half-filling the three interband umklapp terms ($\tilde{g}_{xu}, \tilde{g}_{tu1}, \tilde{g}_{tu2}$) are nonvanishing.

III. RENORMALIZATION GROUP

The Hubbard model values for the coupling constants, obtained from Eq. (2.1), are shown in Table I. To analyze the behavior of the weakly interacting system, we employ the renormalization-group (RG) approach. In the RG, short-wavelength modes are progressively eliminated in a systematic way, leading to differential equations for the renormalized coupling constants which describe the physics of the model at longer and longer length scales. The flow equations for this system in the absence of u_i were first obtained in Ref. 14 using conventional diagrammatic methods. The full set of RG equations is more directly obtained using current algebra, described in more detail in Appendix A. Away from half-filling, they are

$$\begin{aligned}
\dot{g}_{1\rho} = & \beta \left(g_{1\rho}^2 + \frac{3}{16} g_{1\sigma}^2 \right) - \alpha g_{1u}^2, \\
\dot{g}_{2\rho} = & \alpha \left(g_{1\rho}^2 + \frac{3}{16} g_{1\sigma}^2 \right) - \beta g_{2u}^2, \\
\dot{g}_{x\rho} = & - \left(g_{1\rho}^2 + \frac{3}{16} g_{1\sigma}^2 \right), \\
\dot{g}_{1\sigma} = & - \alpha g_{1\sigma}^2 - \frac{\beta}{2} g_{1\sigma}^2 + 2\beta g_{1\rho} g_{1\sigma}, \\
\dot{g}_{2\sigma} = & - \beta g_{2\sigma}^2 - \frac{\alpha}{2} g_{1\sigma}^2 + 2\alpha g_{1\rho} g_{1\sigma}, \\
\dot{g}_{x\sigma} = & - g_{x\sigma}^2 - \frac{1}{2} g_{1\sigma}^2 - 2g_{1\rho} g_{1\sigma}, \dot{g}_{1\rho} = g_{0\rho} g_{1\rho} + \frac{3}{16} g_{0\sigma} g_{1\sigma}, \\
\dot{g}_{1\sigma} = & g_{0\sigma} g_{1\rho} + (g_{0\rho} - g_{0\sigma}/2 - 2g_{x\sigma}) g_{1\sigma}, \\
\dot{g}_{1u} = & - 2\alpha g_{1\rho} g_{1u}, \\
\dot{g}_{2u} = & - 2\beta g_{2\rho} g_{2u}, \quad (3.1)
\end{aligned}$$

where $\tilde{g}_i \equiv \pi(v_1 + v_2)g_i$, $\alpha \equiv (v_1 + v_2)/(2v_1)$, $\beta \equiv (v_1 + v_2)/(2v_2)$, $g_{0\rho} = \alpha g_{1\rho} + \beta g_{2\rho} - 2g_{x\rho}$, and $g_{0\sigma} = \alpha g_{1\sigma}$

The couplings in Eq. (2.6) renormalize ‘‘velocities’’ of various charge and spin modes, and can be neglected to leading order in U for what follows. Additional operators are needed to treat umklapp processes at special dopings:

$+ \beta g_{2\sigma} - 2g_{x\sigma}$. The dots indicate logarithmic derivatives with respect to the length scale, i.e., $\dot{g}_i \equiv \partial g_i / \partial \ell$, where $\ell = \ln L$.

Equations (3.1) are valid until $\max\{g_i\} \sim O(1)$. To analyze them, we employ the following approach. Starting with the appropriate initial values (cf. Table I), we integrate the equations numerically. If, as $\ell \rightarrow \infty$, all the couplings approach finite values, the procedure is controlled, since $\max\{g_i(\ell \rightarrow \infty)\}$ becomes arbitrarily small as $U \rightarrow 0$. If any coupling diverges, we determine the asymptotic behavior of all the couplings with Eqs. (3.1). Specifically, we imagine integrating the flow equations up to a scale ℓ^* , at which point the largest coupling $g_{\text{max}} = \max\{g_i(\ell^*)\}$ satisfies $U/t \ll g_{\text{max}} \ll 1$. This allows us to ignore the higher-order terms [$O(g^3)$] in the RG flow equations. As $U \rightarrow 0$, the rescaling parameter $\ell^* \rightarrow \infty$, so we need only analyze the asymptotic large ℓ behavior of Eq. (3.1).

To do so, we make the ansatz $g_i(\ell) = k g_{i0} / (1 - k\ell)$, where $1/k$ is the scale at which the couplings diverge. Equations (3.1) then reduce to a set of coupled quadratic equations for the $\{g_{i0}\}$. The search for appropriate solutions is considerably aided by the numerical integration of the flow equations. After locating a divergence (which fixes k), we plot $(1 - k\ell)g_i$ versus ℓ , from which g_{i0} is extracted from the intercept with the line $\ell = 1/k$.

Applying this procedure for generic fillings with Hubbard initial values, we found three distinct phases (in the regime with both bands partially filled for $U=0$). For $\alpha \geq 4.8$, the flows are stable, with fixed-point values $g_{1\sigma}^* = g_{x\sigma}^* = g_{2\sigma}^* = g_{1\rho}^* = 0$. When $4.3 \leq \alpha \leq 4.8$, the system is singly unstable, with $g_{2\sigma,0} = -1/\beta$, and all other $g_{i0} = 0$. For more comparable Fermi velocities, $1 < \alpha \leq 4.3$, all the operators except $g_{x\sigma}^* = 0$ diverge, but in such a way that $\alpha g_{1\sigma,0} = \beta g_{2\sigma,0} < 0$ and $g_{1\rho,0} = -1/4g_{1\sigma,0} > 0$. The behavior for $1/2 < \alpha < 1$ is obtained by interchanging band indices in all quantities.

The physics of these phases is elucidated through the use of Abelian bosonization.^{12,10} With the convention $\psi_{R/Li\alpha} \propto \exp(i\sqrt{4\pi}\phi_{R/Li\alpha})$, dual canonical Bose fields may be defined as $\phi_{i\alpha} = \phi_{Ri\alpha} + \phi_{Li\alpha}$ and $\theta_{i\alpha} = \phi_{Ri\alpha} - \phi_{Li\alpha}$. They satisfy $[\phi(x), \theta(y)] = -i \text{sgn}(x-y)/2$. A further canonical transformation to $(\phi, \theta)_{i\rho} = [(\phi, \theta)_{i\uparrow} + (\phi, \theta)_{i\downarrow}]/\sqrt{2}$ and $(\phi, \theta)_{i\sigma} = [(\phi, \theta)_{i\uparrow} - (\phi, \theta)_{i\downarrow}]/\sqrt{2}$ yields the spin-charge-separated Euclidean action

$$S_0 = \sum_{i\nu} \int_{x,\tau} \frac{v_i}{2} [(\partial_x \phi_{i\nu})^2 + (\partial_x \theta_{i\nu})^2] + i \partial_x \theta_{i\nu} \partial_\tau \phi_{i\nu}, \quad (3.2)$$

where $\nu = \rho, \sigma$. Using the scheme discussed in the Introduction, the noninteracting system with both bands occupied [Eq. (3.2)] is classified as C2S2. The large α phase found above is also of C2S2-type, though it contains the additional (marginal) couplings $g_{i\rho}, g_{x\rho}, \lambda_{i\rho}, \lambda_{x\rho}, \lambda_{i\sigma}$, and $\lambda_{x\sigma}$, which makes the behavior highly nonuniversal.¹⁶

In the intermediate state ($4.3 \leq \alpha \leq 4.8$), $g_{2\sigma}$ becomes large and negative. Using bosonization, this interaction (neglecting unimportant gradient terms) is

$$S_{2\sigma} \propto \tilde{g}_{2\sigma} \int_{x,\tau} M^2 \cos(\sqrt{8\pi}\theta_{2\sigma}), \quad (3.3)$$

where the coefficient M is cutoff dependent. In the scaling limit, it is appropriate to expand the cosine and obtain a true mass M for $\theta_{2\sigma}$. The resulting phase is therefore C2S1. For $\alpha \leq 4.3$, an analogous cosine appears in the 1σ sector, and the asymptotic divergence of $g_{i\rho}$ and $g_{i\sigma}$ is such that the interband hopping terms sum to

$$S_i \propto \tilde{g}_{i\rho} \int_{x,\tau} \cos(\sqrt{4\pi}\phi_{-\rho}) \cos(\sqrt{2\pi}\theta_{1\sigma}) \cos(\sqrt{2\pi}\theta_{2\sigma}), \quad (3.4)$$

where $\phi_{\pm\rho} \equiv (\phi_{1\rho} \pm \phi_{2\rho})/\sqrt{2}$. It is natural to assign masses to $\theta_{1\sigma}$ and $\theta_{2\sigma}$, after which Eq. (3.4) acts to fix $\phi_{-\rho} = \sqrt{\pi}/2$ (up to gapped fluctuations), since $\tilde{g}_{i\rho} > 0$. Note that $\sqrt{4\pi}\phi_{-\rho}$ appears as the phase difference between pairing operators in the bonding and antibonding bands, so that this value of $\phi_{-\rho}$ leads to $\langle \psi_{1\uparrow} \psi_{1\downarrow} (\psi_{2\uparrow} \psi_{2\downarrow})^\dagger \rangle < 0$. A natural definition of ‘‘ d -wave’’ in this context is just $\langle e^{i\sqrt{4\pi}\phi_{-\rho}} \rangle < 0$. The resulting state has only a single ungapped charge mode (with dual fields $\theta_{+\rho}, \phi_{+\rho}$), and will be labeled C1S0. It may be characterized by a single dimensionless stiffness $K_{+\rho}$ and a velocity $v_{+\rho}$, such that the effective action for $\theta_{+\rho}$ is

$$S_{+\rho} = \frac{K_{+\rho}}{2} \int_{x,\tau} \{v_{+\rho} (\partial_x \theta_{+\rho})^2 + v_{+\rho}^{-1} (\partial_\tau \theta_{+\rho})^2\}, \quad (3.5)$$

with a similar dual ($K_{+\rho} \rightarrow K_{+\rho}^{-1}$) form for $\phi_{+\rho}$. Equation (3.5) interpolates smoothly between a CDW (at large $K_{+\rho}$) and a superconductor (at small $K_{+\rho}$). The pairing exponent $\kappa = K_{+\rho}/2$, while the CDW-like correlator $\langle n^2(x)n^2(0) \rangle_c \sim \cos[2(k_{F1} + k_{F2})x]/x^{2/K_{+\rho}}$, plus power laws ($1/x^2$) at $k=0$. We are unable to determine $K_{+\rho}$ and $v_{+\rho}$ in a controlled way, because they depend on the entire crossover from the noninteracting state to the C1S0 fixed line (see Appendix B). However, heuristic calculations suggest that superconducting fluctuations ($K_{+\rho}^{-1}$) increase with increasing $v_1 - v_2$. Interestingly, the usual power-law term at $2k_F$ is missing from the density-density correlation function in the C1S0 phase, as noted by Nagaosa⁸ in a similar model, due to strong fluctuations of the $\theta_{-\rho}$ and $\phi_{i\sigma}$ fields.

It remains to discuss the behavior at several ‘‘special’’ points in the phase diagram. When $k_{F2} = \pi/2$, umklapp processes imply $g_{2u} \neq 0$. For $t_\perp > t$, this occurs with band 1 empty, and one gets the usual C0S1 spin-density wave, as

shown in Fig. 1. For $t_\perp < t$, we must consider interband coupling via Eqs. (3.1). For almost all ratios of the velocities, we find that a charge gap develops in band 2, simultaneously suppressing the other potential instabilities, leading to a C1S2 phase. Surprisingly, over the narrow range $0.6 \leq \beta \leq 0.85$, g_{2u} renormalizes to zero, yielding instead the C1S0 state (see Fig. 1). The behavior at half-filling is more difficult to obtain, because it requires the inclusion of the g_{xu}, g_{tu1} , and g_{tu2} operators in Eq. (2.7). The RG equations in this case are given in Appendix A. Their analysis indicates a completely gapped (C0S0) phase, as suggested by a large U picture of coupled antiferromagnetic Heisenberg chains.¹⁵

The final remaining special point occurs when the Fermi level lies precisely at the bottom of band 1. It is outside the scope of conventional RG’s, because the dispersion in band 1 is quadratic, with the Hamiltonian

$$H_1 = - \int \frac{1}{x} \frac{1}{2m\epsilon} \psi_1^\dagger \partial_x^{1+\epsilon} \psi_1, \quad (3.6)$$

where $\epsilon = 1$ for the quadratic band, but must be taken as a small parameter to control the perturbative treatment. The allowed couplings are $g_{2\rho}, g_{2\sigma}, \lambda_{2\rho}$, and the four interband terms

$$- \mathcal{H}_{1-2} = \tilde{u}_\rho (J_{R2} + J_{L2}) J_1 + \tilde{u}_\sigma (\mathbf{J}_{R2} + \mathbf{J}_{L2}) \cdot \mathbf{J}_1 - \frac{\tilde{v}}{2} J_1^2 - \tilde{u}_i (\psi_{R2\alpha}^\dagger \psi_{L2\beta}^\dagger \psi_{1\beta} \psi_{1\alpha} + \text{H.c.}), \quad (3.7)$$

where $J_1 = \psi_{1\alpha}^\dagger \psi_{1\alpha}$ and $\mathbf{J}_1 = \psi_{1\alpha}^\dagger \boldsymbol{\sigma}_{\alpha\beta} \psi_{1\beta}/2$. The RG equations in this case must be derived via conventional diagrammatic techniques (see, e.g., Ref. 14), since current algebra methods rely on having a linear spectrum at the Fermi energy. They are

$$\dot{g}_{2\rho} = u_i^2/2, \quad \dot{g}_{2\sigma} = -g_\sigma^2 - 2u_i^2, \quad \dot{u}_\rho = \gamma m^{-\epsilon} u_i^2,$$

$$\dot{u}_\sigma = -\gamma u_\sigma^2, \quad \dot{v} = \epsilon v - 2v^2 - u_i^2,$$

$$\dot{u}_i = (\epsilon/2 - 2v - 4\gamma u_\rho - 3g_\sigma/4 + g_\rho) u_i, \quad (3.8)$$

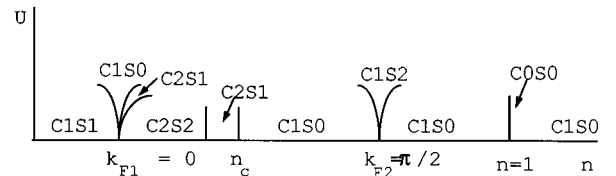


FIG. 3. Cut through the phase diagram at constant t_\perp . Note that two of the lines in Fig. 1 associated with special fillings have broadened into fans for finite U . The vertical line at $n=1$ (half-filling) does not broaden, because it corresponds to the exact point of particle-hole symmetry of the original Hubbard Hamiltonian.

where $m = 2\tilde{m}^\epsilon$, $\gamma = 1/(1 + m^{-\epsilon})$, $u_t = m^{\epsilon/2}\tilde{u}_t$, $v = m^\epsilon\tilde{v}/(4\pi)$, $(g_2, u)_{\rho, \sigma} = (\tilde{g}_2, \tilde{u})_{\rho, \sigma}/(2\pi v_2)$ (we have taken a momentum cutoff of 1). Because of the relative simplicity of Eqs. (3.8), we have been able to analytically show an instability for Hubbard initial conditions.¹⁵ Analysis of the flow asymptotics indicates that at this special point, fluctuation-induced attractive interactions $v < 0$ in band 1 populate it with spinless bound pairs. Simultaneously, $g_{2\sigma} < 0$ creates a spin gap in band 2, and u_t Josephson couples the two bands, gapping the out of phase charge mode to leave a C1S0 phase. This RG analysis holds for $U \ll \epsilon \ll 1$, but we expect the tendency to pairing to *increase* with ϵ , due to the increased density of states for interband scattering. Physically, the presence of the C1S0 phase at $k_{F1} = 0$ can be attributed to the Van Hove singularity at the band edge. Note that this Van Hove mechanism also leads to “*d-wave*”-like pairing, in the sense that the interband pair hopping interaction (u_t) remains repulsive, encouraging $\langle \psi_{1\uparrow}\psi_{1\downarrow}(\psi_{2\uparrow}\psi_{2\downarrow})^\dagger \rangle < 0$, as in the other C1S0 phase.

The above results at special fillings are valid only at isolated points for infinitesimal U . For finite U , the RG suggests that the regions of attraction of these phases widen into fans of width $\delta t_\perp \sim \exp(-ct/U)$, where c is a constant. The nonuniformity of Eqs. (3.8) allows for additional structure within the fan. In particular, because the instability is driven by the $g_{2\sigma}$ term, we expect a narrow intermediate wedge of C2S1, as shown in Fig. 3. In the future, it will be interesting to generalize these calculations to three-chain systems ($N=3$), to help clarify which features are particular to even N .

IV. COMPARISON WITH PREVIOUS WORK

Problems of coupled Luttinger liquids have been investigated previously by many authors. Indeed, our RG equations for generic fillings were calculated by Varma and Zawadowski in Ref. 14. These authors noted the existence of an instability in a large range of parameters. Using purely RG methods, without the benefit of the organization of a current algebra description or the interpretation allowed by bosonization, they did not identify the nature of the C1S0 phase. Other authors have also noted the enhancement of pair tunneling processes.¹⁸

Some years later, Penc and Sólyom¹⁹ (PS) calculated the two-loop (cubic-order) RG equations, which exhibit fixed points instead of instabilities. Because these fixed points occur at values of the coupling constants of order one, however, the calculation of properties from these fixed point values is *uncontrolled*. Indeed, experience with bosonization leads us to believe that the instabilities at the one-loop level signal the development of various gaps, which cannot be captured within such a description.

An approach much closer to our own was taken by Fabrizio,¹⁰ who employed bosonization to rewrite the effective Hamiltonian of the putative fixed points of PS. These fixed point forms contain the same cosine terms found above [Eqs. (3.3)–(3.4)], which allowed Fabrizio to postulate an appropriate set of gaps for the phases he found. Three of the phases in his phase diagram (Fig. 9 of Ref. 10) correspond to ours: LL1, which is our C1S1; LL2, our C2S2 state; and I, our C1S0 phase.

We note, however, that the assignment of a particular phase to a particular set of Hubbard parameters based on the PS fixed points is *incorrect*. Indeed, a detailed comparison with our results shows a disagreement in the location of the phase boundaries, and, more seriously, the complete absence of the C2S1 phase. In addition, using the full PS equations at large U , Fabrizio finds two extra phases (denoted II and III). As we have emphasized, however, these fixed points (particularly strong-coupling ones) have no particular physical significance, and the existence of additional strong-coupling phases is questionable.

Our approach does not make use of these unphysical fixed points, and relies only on the small-coupling results of the RG. Instead, we have *matched* the asymptotic form of the weak-coupling instabilities to the possible (inherently strong-coupling) phases which are characterized by various gaps. The nature of the RG instabilities are entirely contained in the one-loop RG equations, and because the two-loop corrections obtained by PS are small in this regime, they need not be included in the calculation (see the discussion in Sec. III).

ACKNOWLEDGMENTS

We are grateful to A. Ludwig and especially D. Scalapino for innumerable fruitful discussions. This work has been supported by the National Science Foundation under Grants No. PHY89-04035 and No. DMR-9400142.

Note added in proof. Recent work with Lin²⁰ has discovered a *very weak instability* of the asymptotics leading to the C1S0 phase. This implies that, in the *extreme* weak coupling limit, $U/t < 10^{-5}$, the C2S1 phase expands to fill the majority of the C1S0 region in Fig. 1. In this limit, the C1S0 phase persists only in a narrow sliver near half-filling. For small but noninfinitesimal coupling, $10^{-5} < U/t \ll 1$, however, the asymptotic analysis leading to the phase diagram in Fig. 1 is correct, and the main conclusions of the text are unchanged.

APPENDIX A: CURRENT ALGEBRA

Current algebra methods allow, among other things, an *algebraic* calculation of the one-loop RG equations. It is discussed in some depth in Ref. 17. Here we give a very terse description of the method, stressing the new points of our calculation. All the currents are defined in terms of the fermion fields $\psi_{R/La\alpha}$ ($a=1,2$), which obey the operator products

$$\begin{aligned} \psi_{Ra\alpha}(x, \tau) \psi_{Rb\beta}^\dagger(0, 0) &\sim \frac{\delta_{ab} \delta_{\alpha\beta}}{2\pi z_a} + O(1), \\ \psi_{La\alpha}(x, \tau) \psi_{Lb\beta}^\dagger(0, 0) &\sim \frac{\delta_{ab} \delta_{\alpha\beta}}{2\pi z_a^*} + O(1), \end{aligned} \quad (\text{A1})$$

where $z_a = v_a \tau - ix$. The operators products should be understood to hold when two points (x, τ) and $(0, 0)$ are brought close together, as replacements within correlation functions. Equations (1.1) allow a simple calculation of the operator products of the currents defined in Eq. (2.4). As an example, consider the product $J_{R1}^i J_{R1}^j$. Performing all possible contractions gives

$$J_{1R}^i(z_1)J_{1R}^j(0,0) \sim : \psi_{1R\alpha}^\dagger(z_1)\psi_{1R\beta}(z_1) :: \psi_{1R\gamma}^\dagger(0)\psi_{1R\epsilon}(0) : \frac{1}{4} \sigma_{\alpha\beta}^i \sigma_{\gamma\epsilon}^j \quad (\text{A2})$$

$$\begin{aligned} & \sim \left[- \left(\frac{-1}{2\pi z_1} \right) \left(\frac{1}{2\pi z_1} \right) \delta_{\alpha\epsilon} \delta_{\beta\gamma} + \frac{\delta_{\beta\gamma}}{2\pi z_1} : \psi_{1R\alpha}^\dagger \psi_{1R\epsilon} : + \frac{\delta_{\alpha\epsilon}}{2\pi z_1} : \psi_{1R\beta} \psi_{1R\gamma} : + : \psi_{1R\alpha}^\dagger \psi_{1R\beta} \psi_{1R\gamma}^\dagger \psi_{1R\epsilon} : \right] \frac{1}{4} \sigma_{\alpha\beta}^i \sigma_{\gamma\epsilon}^j \\ & \sim \frac{1/2}{(2\pi z_1)^2} \delta^{ij} + \frac{1}{2\pi z_1} i \epsilon^{ijk} J_{1R}^k + O(1). \end{aligned} \quad (\text{A3})$$

Note that the structure arises as a result of extending the normal-ordering ($:$) symbol to the full product. To perform the final simplification, we used the relation $\sigma^i \sigma^j = \delta^{ij} + i \epsilon^{ijk} \sigma^k$. Computation of the full set of operator products is equally simple (though tedious). The ones needed away from 1/2 filling are

$$J_{aR} J_{bR} \sim \frac{2}{(2\pi z_a)^2} \delta_{ab}, \quad (\text{A4})$$

$$J_{aR}^i J_{bR}^j \sim \left[\frac{1/2}{(2\pi z_a)^2} \delta^{ij} + \frac{1}{2\pi z_a} i \epsilon^{ijk} J_{aR}^k \right] \delta_{ab}, \quad (\text{A5})$$

$$L_R L_R^\dagger \sim \frac{2}{(2\pi)^2 z_1 z_2} + \frac{J_{1R}}{2\pi z_2} - \frac{J_{2R}}{2\pi z_1}, \quad (\text{A6})$$

$$\begin{aligned} L_R^i L_R^{j\dagger} & \sim \frac{1/2 \delta^{ij}}{(2\pi)^2 z_1 z_2} + \frac{i}{2} \epsilon^{ijk} \left(\frac{J_{1R}^k}{2\pi z_2} + \frac{J_{2R}^k}{2\pi z_1} \right) \\ & + \frac{1}{4} \delta^{ij} \left(\frac{J_{1R}}{2\pi z_2} - \frac{J_{2R}}{2\pi z_1} \right), \end{aligned} \quad (\text{A7})$$

$$L_R^i L_R^{\dagger j} \sim \frac{J_{1R}^i}{2\pi z_2} - \frac{J_{2R}^j}{2\pi z_1}, \quad (\text{A8})$$

$$L_R J_{aR} \sim (-1)^a \frac{1}{2\pi z_a} L_R, \quad (\text{A9})$$

$$L_R^\dagger J_{aR} \sim (-1)^{a+1} \frac{1}{2\pi z_a} L_R^\dagger, \quad (\text{A10})$$

$$L_R J_{aR}^i \sim (-1)^a \frac{1}{2\pi z_a} L_R^i, \quad (\text{A11})$$

$$L_R^\dagger J_{aR}^i \sim (-1)^{a+1} \frac{1}{2\pi z_a} L_R^{i\dagger}, \quad (\text{A12})$$

$$L_R^i J_{aR} \sim (-1)^a \frac{1}{2\pi z_a} L_R^i, \quad (\text{A13})$$

$$L_R^{i\dagger} J_{aR} \sim (-1)^{a+1} \frac{1}{2\pi z_a} L_R^{i\dagger}, \quad (\text{A14})$$

$$L_R^i J_{aR}^j \sim \frac{1}{2\pi z_a} \left[\frac{i}{2} \epsilon^{ijk} L_R^k + (-1)^a \frac{1}{4} \delta^{ij} L_R \right], \quad (\text{A15})$$

$$L_R^{i\dagger} J_{aR}^j \sim \frac{1}{2\pi z_a} \left[\frac{i}{2} \epsilon^{ijk} L_R^{k\dagger} - (-1)^a \frac{1}{4} \delta^{ij} L_R^\dagger \right], \quad (\text{A16})$$

$$M_{aR} M_{bR}^\dagger \sim \left[\frac{1}{(2\pi z_a)^2} - \frac{J_{aR}}{2\pi z_a} \right] \delta_{ab}, \quad (\text{A17})$$

$$M_{aR} J_{bR} \sim \frac{2\delta_{ab}}{2\pi z_a} M_{aR}, \quad (\text{A18})$$

$$M_{aR}^\dagger J_{bR} \sim -\frac{2\delta_{ab}}{2\pi z_a} M_{aR}^\dagger, \quad (\text{A19})$$

where the coordinates of the two operators on each left-hand side are consecutively (x, τ) and $(0, 0)$. The operator products $M_{aR} L_R$ and $M_{aR}^\dagger L_R^\dagger$ are also nonvanishing, but do not enter in the one-loop RG away from half-filling (but see below). Similar forms hold for the left-moving currents, but with $z_a \rightarrow z_a^*$.

The renormalization-group equations are obtained very simply from Eqs. (A4)–(A19). We use the functional integral formulation, in which the terms of Eq. (2.5) appear as interactions in an Euclidean action, $S_E = \int dx d\tau \mathcal{H}$, and

$$\mathcal{Z} = \int [d\bar{\psi}][d\psi] e^{-S_E}. \quad (\text{A20})$$

To perform the RG, the exponential is expanded to quadratic order in \mathcal{H}_{int} . A typical term takes the form

$$\frac{\tilde{g}_{1\sigma}^2}{2} \int_{z,w} \langle J_{1R}^i(z) J_{1L}^i(z) J_{1R}^j(w) J_{1L}^j(w) \rangle, \quad (\text{A21})$$

where $\int_{z,w}$ denotes a four-dimensional integral over the two complex planes z and w . As in any RG, we wish to integrate out the short-scale degrees of freedom to derive the effective theory at long wavelengths and low energies. Here this is accomplished by considering the contributions to Eq. (A21) when the two points z and w are close together (near the cutoff scale). It is then appropriate to employ the operator product expansion, which gives

$$\frac{\tilde{g}_{1\sigma}^2}{2} i \epsilon^{ijk} i \epsilon^{ijl} \int_{z,w} \frac{1}{2\pi(z_1 - w_1)} \frac{1}{2\pi(z_1^* - w_1^*)} J_{1R}^k J_{1L}^l. \quad (\text{A22})$$

At this stage, it is necessary to more carefully specify the cutoff prescription. We will choose a short-distance cutoff a in space, but none in imaginary time. For a rescaling factor b , we must then perform the integral

$$I_1 = \int_{a < |x| < ba} dx \int_{-\infty}^{\infty} d\tau \frac{1}{(2\pi)^2 (v_1^2 \tau^2 + x^2)} = \frac{\ln b}{2\pi v_1} \quad (\text{A23})$$

over the relative coordinates (x, τ) . Using Eq. (A23) in Eq. (A22) gives

$$-\frac{\tilde{g}_{1\sigma}^2}{2\pi v_1} \ln b \int_z \mathbf{J}_{1R} \cdot \mathbf{J}_{1L}, \quad (\text{A24})$$

which, when re-exponentiated, renormalizes $\tilde{g}_{1\sigma}$, and for $b = e^{d\ell}$ gives the first term in the flow equation for $g_{1\sigma}$ in Eq. (3.1). Similar calculations for the remaining terms result in the denominators $|z_1 - w_1|^2$, $|z_2 - w_2|^2$, and $(z_1 - w_1)(z_2^* - w_2^*)$, which yield the factors $1/(2\pi v_1)$, $1/(2\pi v_2)$, and $1/[\pi(v_1 + v_2)]$, respectively, and thereby lead to the α and β factors in Eqs. (3.1). All other forms appearing in the integrals over the relative coordinates give zero contribution, reflecting causality of the ballistic fermion propagators.

For the special case of half-filling, additional operator products are required. To simplify the analysis, we note, however, that at half-filling, the two velocities are equal, $v_1 = v_2 \equiv v$. It is therefore not necessary in this case to differentiate between $z_1 = z_2 \equiv z$. Making this assumption, the new relations are

$$N_{R\alpha\beta} N_{R\gamma\epsilon}^\dagger \sim + \frac{\delta_{\alpha\gamma} \delta_{\beta\epsilon}}{(2\pi z)^2} - \frac{\delta_{\alpha\gamma} \delta_{\beta\epsilon}}{4\pi z} (\mathbf{J}_{1R} + \mathbf{J}_{2R}) \quad (\text{A25})$$

$$- \frac{1}{2\pi z} [\delta_{\alpha\gamma} \mathbf{J}_{2R} \cdot \boldsymbol{\sigma}_{\epsilon\beta} + \delta_{\beta\epsilon} \mathbf{J}_{1R} \cdot \boldsymbol{\sigma}_{\gamma\alpha}],$$

$$N_{R\alpha\beta} \mathbf{J}_{aR} \sim \frac{1}{2\pi z} N_{R\alpha\beta},$$

$$N_{R\alpha\beta}^\dagger \mathbf{J}_{aR} \sim - \frac{1}{2\pi z} N_{R\alpha\beta}^\dagger,$$

$$N_{R\alpha\beta} \mathbf{J}_{1R} \sim \frac{1}{2\pi z} \frac{\boldsymbol{\sigma}_{\alpha\gamma}}{2} N_{R\gamma\beta},$$

$$N_{R\alpha\beta} \mathbf{J}_{2R} \sim \frac{1}{2\pi z} \frac{\boldsymbol{\sigma}_{\beta\gamma}}{2} N_{R\alpha\gamma},$$

$$N_{R\alpha\beta}^\dagger \mathbf{J}_{1R} \sim - \frac{1}{2\pi z} \frac{\boldsymbol{\sigma}_{\gamma\alpha}}{2} N_{R\gamma\beta}^\dagger,$$

$$N_{R\alpha\beta}^\dagger \mathbf{J}_{2R} \sim - \frac{1}{2\pi z} \frac{\boldsymbol{\sigma}_{\gamma\beta}}{2} N_{R\alpha\gamma}^\dagger,$$

$$N_{R\alpha\beta} L_R \sim - \frac{1}{2\pi z} \boldsymbol{\sigma}_{\alpha\beta}^y M_{2R},$$

$$N_{R\alpha\beta}^\dagger L_R \sim - \frac{1}{2\pi z} \boldsymbol{\sigma}_{\alpha\beta}^y M_{1R}^\dagger,$$

$$N_{R\alpha\beta} L_R^\dagger \sim - \frac{1}{2\pi z} \boldsymbol{\sigma}_{\alpha\beta}^y M_{1R},$$

$$N_{R\alpha\beta}^\dagger L_R^\dagger \sim - \frac{1}{2\pi z} \boldsymbol{\sigma}_{\alpha\beta}^y M_{2R}^\dagger,$$

$$N_{R\alpha\beta} L_R \sim - \frac{1}{2\pi z} \frac{(\boldsymbol{\sigma}\boldsymbol{\sigma}^y)_{\alpha\beta}}{2} M_{2R},$$

$$N_{R\alpha\beta}^\dagger L_R \sim - \frac{1}{2\pi z} \frac{(\boldsymbol{\sigma}^y \boldsymbol{\sigma})_{\alpha\beta}}{2} M_{1R}^\dagger,$$

$$N_{R\alpha\beta} L_R^\dagger \sim \frac{1}{2\pi z} \frac{(\boldsymbol{\sigma}\boldsymbol{\sigma}^y)_{\alpha\beta}}{2} M_{1R},$$

$$N_{R\alpha\beta}^\dagger L_R^\dagger \sim \frac{1}{2\pi z} \frac{(\boldsymbol{\sigma}^y \boldsymbol{\sigma})_{\alpha\beta}}{2} M_{2R}^\dagger,$$

$$M_{1R} L_R \sim \frac{\boldsymbol{\sigma}_{\alpha\beta}^y}{2\pi z} N_{R\alpha\beta},$$

$$M_{1R}^\dagger L_R^\dagger \sim \frac{\boldsymbol{\sigma}_{\alpha\beta}^y}{2\pi z} N_{R\alpha\beta}^\dagger,$$

$$M_{2R} L_R \sim \frac{\boldsymbol{\sigma}_{\alpha\beta}^y}{2\pi z} N_{R\alpha\beta},$$

$$M_{2R}^\dagger L_R^\dagger \sim \frac{\boldsymbol{\sigma}_{\alpha\beta}^y}{2\pi z} N_{R\alpha\beta}^\dagger,$$

$$M_{1R} L_R \sim \frac{1}{2\pi z} \frac{(\boldsymbol{\sigma}^y \boldsymbol{\sigma})_{\alpha\beta}}{2} N_{R\alpha\beta},$$

$$M_{1R}^\dagger L_R^\dagger \sim - \frac{1}{2\pi z} \frac{(\boldsymbol{\sigma}\boldsymbol{\sigma}^y)_{\alpha\beta}}{2} N_{R\alpha\beta}^\dagger,$$

$$M_{2R} L_R \sim - \frac{1}{2\pi z} \frac{(\boldsymbol{\sigma}^y \boldsymbol{\sigma})_{\alpha\beta}}{2} N_{R\alpha\beta},$$

$$M_{2R}^\dagger L_R^\dagger \sim \frac{1}{2\pi z} \frac{(\boldsymbol{\sigma}\boldsymbol{\sigma}^y)_{\alpha\beta}}{2} N_{R\alpha\beta}^\dagger,$$

$$M_{1R} N_{R\alpha\beta}^\dagger \sim - \frac{1}{2\pi z} \left[\frac{\boldsymbol{\sigma}_{\alpha\beta}^y}{2} L_R^\dagger + L_R^\dagger \cdot (\boldsymbol{\sigma}^y \boldsymbol{\sigma})_{\alpha\beta} \right],$$

$$M_{1R}^\dagger N_{R\alpha\beta} \sim - \frac{1}{2\pi z} \left[\frac{\boldsymbol{\sigma}_{\alpha\beta}^y}{2} L_R - L_R \cdot (\boldsymbol{\sigma}\boldsymbol{\sigma}^y)_{\alpha\beta} \right],$$

$$M_{2R} N_{R\alpha\beta}^\dagger \sim - \frac{1}{2\pi z} \left[\frac{\boldsymbol{\sigma}_{\alpha\beta}^y}{2} L_R - L_R \cdot (\boldsymbol{\sigma}^y \boldsymbol{\sigma})_{\alpha\beta} \right],$$

$$M_{2R}^\dagger N_{R\alpha\beta} \sim - \frac{1}{2\pi z} \left[\frac{\boldsymbol{\sigma}_{\alpha\beta}^y}{2} L_R^\dagger + L_R^\dagger \cdot (\boldsymbol{\sigma}\boldsymbol{\sigma}^y)_{\alpha\beta} \right].$$

With these operator products, a full set of RG equations can be derived at half-filling, using the previously described procedure. After some lengthy algebra, one finds

$$\begin{aligned}
\dot{g}_{1\rho} &= g_{t\rho}^2 + \frac{3}{16}g_{t\sigma}^2 - g_{tu1}^2 - g_{tu1}g_{tu2} - g_{tu2}^2, \\
\dot{g}_{x\rho} &= -g_{t\rho}^2 - \frac{3}{16}g_{t\sigma}^2 - g_{tu1}^2 - g_{tu1}g_{tu2} - g_{tu2}^2 - g_{xu}^2, \\
\dot{g}_{1\sigma} &= 2g_{t\rho}g_{t\sigma} - \frac{1}{2}g_{t\sigma}^2 - 4g_{tu1}^2 - 4g_{tu1}g_{tu2} - g_{1\sigma}^2, \\
\dot{g}_{x\sigma} &= -2g_{t\rho}g_{t\sigma} - \frac{1}{2}g_{t\sigma}^2 - 4g_{tu1}g_{tu2} - 4g_{tu2}^2 - g_{x\sigma}^2, \\
\dot{g}_{t\rho} &= g_{0\rho}g_{t\rho} + \frac{3}{16}g_{0\sigma}g_{t\sigma} - g_{xu}(g_{tu1} - g_{tu2}), \\
\dot{g}_{t\sigma} &= g_{0\sigma}g_{t\rho} + \left(g_{0\rho} - \frac{1}{2}g_{0\sigma} - 2g_{x\sigma} \right) g_{t\sigma} \\
&\quad + 4g_{xu}(g_{tu1} + g_{tu2}), \\
\dot{g}_{xu} &= - \left(2g_{t\rho} - \frac{3}{2}g_{t\sigma} \right) g_{tu1} \\
&\quad + \left(2g_{t\rho} + \frac{3}{2}g_{t\sigma} \right) g_{tu2} - 4g_{x\rho}g_{xu}, \\
\dot{g}_{tu1} &= -(2g_{t\rho} - g_{t\sigma}/2)g_{xu} - g_{tu2}g_{1\sigma} \\
&\quad - g_{tu1} \left(2g_{x\rho} - \frac{1}{2}g_{x\sigma} + 2g_{1\rho} + \frac{3}{2}g_{1\sigma} \right), \\
\dot{g}_{tu2} &= -g_{tu1}g_{x\sigma} + (2g_{t\rho} + g_{t\sigma}/2)g_{xu} \\
&\quad - g_{tu2} \left(2g_{x\rho} + \frac{3}{2}g_{x\sigma} + 2g_{1\rho} - \frac{1}{2}g_{1\sigma} \right), \quad (\text{A26})
\end{aligned}$$

where we have assumed, as dictated by chain-interchange symmetry, that $g_{1\rho} = g_{2\rho}$ and $g_{1\sigma} = g_{2\sigma}$, and that, as is the case for generic t_\perp , $g_{1u} = g_{2u} = 0$.

APPENDIX B: STIFFNESS OF THE C1S0 PHASE

In this appendix, we attempt to compute the stiffness $K_{+\rho}$ in the C1S0 phase, by following the RG flows and usual standard ‘‘matching’’ procedures. We find, however, that for $v_1 \neq v_2$, the value of $K_{+\rho}$ depends on the details of this crossover, and hence is not accessible by the present method.

Our strategy is to integrate Eqs. (3.1) until the diverging couplings are order 1 in the renormalized action. It is then justified to assign gaps to the appropriate fields and simply integrate out the massive modes. In the C1S0 phase, we need only consider the charge sector: both spin modes are gapped, and may be integrated out without affecting the long-wavelength properties of the charge modes. From the asymptotic analysis of Sec. III, we know that the remaining [$O(1)$] interactions take the form

$$\begin{aligned}
\mathcal{H}_{\text{int}} &= -\tilde{\Gamma} [\beta J_{1R} J_{1L} + \alpha J_{2R} J_{2L} - J_{1R} J_{2L} - J_{2R} J_{1L} \\
&\quad - g \cos(\sqrt{4\pi} \phi_{-\rho})], \quad (\text{B1})
\end{aligned}$$

where $\tilde{\Gamma} > 0$ and $g > 0$ are $O(1)$ constants. It is crucial to note that $\tilde{\Gamma}$ is not precisely known. It depends upon the point at which one stops integrating the perturbative flow equations. This reflects the fact that what one really wishes to do is calculate crossover properties from the unstable fixed point at $U=0$ to the final C1S0 fixed line. Some such crossover properties may require a knowledge of the RG flows along the entire trajectory between these fixed spaces. We will see that this is the case for $K_{+\rho}$.

From Eq. (2.1), we may easily derive the bosonized representation of the charge sector of the action. Following the notation introduced in the text, one finds

$$\begin{aligned}
S_\rho &= \frac{1}{2} \int dx d\tau \left\{ \sum_{\nu=\pm} \left([\bar{\nu} - \Gamma(\alpha + \beta - 2\nu)] (\partial_x \theta_{\nu\rho})^2 + [\bar{\nu} + \Gamma(\alpha + \beta - 2\nu)] (\partial_x \phi_{\nu\rho})^2 \right) + [\Delta - 2\Gamma(\beta - \alpha)] \partial_x \theta_{+\rho} \partial_x \theta_{-\rho} \right. \\
&\quad \left. + [\Delta + 2\Gamma(\beta - \alpha)] \partial_x \phi_{+\rho} \partial_x \phi_{-\rho} + 2i \partial_\tau \theta_{+\rho} \partial_x \phi_{+\rho} + 2i \partial_\tau \theta_{-\rho} \partial_x \phi_{-\rho} + 4\pi\Gamma g \cos(\sqrt{4\pi} \phi_{-\rho}) \right\}, \quad (\text{B2})
\end{aligned}$$

where $\bar{\nu} = (v_1 + v_2)/2$, $\Delta = v_1 - v_2$, and $\Gamma = \tilde{\Gamma}/(2\pi)$. In the renormalized theory with Γg of order 1, it is legitimate to expand the cosine around its minimum value: $\phi_{-\rho} = \sqrt{\pi}/2 + \sigma$. Integrating out the σ field effectively removes all terms containing $\phi_{-\rho}$ in Eq. (2.2) (only irrelevant Laplacian-squared-type couplings are generated). The $\theta_{+\rho}$ field is isolated by integrating out the $\theta_{-\rho}$ and $\phi_{+\rho}$ fields to yield

$$\begin{aligned}
S_{+\rho} &= \frac{1}{2} \int dx d\tau \left\{ \left[\bar{\nu} + \Gamma(2 - \alpha - \beta) - \frac{1}{4} \frac{[\Delta - 2\Gamma(\beta - \alpha)]^2}{\bar{\nu} - \Gamma(\alpha + \beta + 2)} \right] \right. \\
&\quad \left. \times (\partial_x \theta_{+\rho})^2 + \frac{1}{\bar{\nu} - \Gamma(2 - \alpha - \beta)} (\partial_\tau \theta_{+\rho})^2 \right\}. \quad (\text{B3})
\end{aligned}$$

Comparison with Eq. (3.5) gives

$$K_{+\rho}^2 = \left(\bar{v} - \Gamma(\alpha + \beta - 2) - \frac{1}{4} \frac{[\Delta - 2\Gamma(\beta - \alpha)]^2}{\bar{v} - \Gamma(\alpha + \beta + 2)} \right) \times \frac{1}{\bar{v} - \Gamma(2 - \alpha - \beta)}. \quad (\text{B4})$$

Note that $K_{+\rho}$ depends on Γ , as promised. We note, however, a trend: assuming Γ is roughly constant as v_1 and v_2 are varied, SC correlations are enhanced (i.e., $K_{+\rho}$ is reduced) for increasing $v_1 - v_2$.

¹See, e.g., H. J. Schulz, *Int. J. Mod. Phys* **5**, 57 (1991).

²E. Dagotto, J. Riera, and D. Scalapino, *Phys. Rev. B* **45**, 5744 (1992); T. M. Rice, S. Gopalan, and M. Sigrist, *Europhys. Lett.* **23**, 445 (1993); R. S. Eccleston *et al.*, *Phys. Rev. Lett.* **73**, 2626 (1994); M. Azuma *et al.*, *ibid.* **73**, 3463 (1994).

³D. G. Clarke, S. P. Strong, and P. W. Anderson, *Phys. Rev. Lett.* **72**, 3218 (1994).

⁴H. J. Schulz (unpublished).

⁵A. M. Finkelstein and A. I. Larkin, *Phys. Rev. B* **47**, 10 461 (1993).

⁶D. V. Khveshchenko and T. M. Rice, *Phys. Rev. B* **50**, 272 (1994).

⁷K. Kuroki and H. Aoki, *Phys. Rev. Lett.* **72**, 2947 (1994).

⁸N. Nagaosa, *Solid State Commun.* **94**, 495 (1995).

⁹R. M. Noack, S. R. White, and D. J. Scalapino, *Phys. Rev. Lett.* **73**, 882 (1994); and *Europhys. Lett.* **30**, 163 (1995); D. Poilblanc, D. J. Scalapino, and W. Hanke, *Phys. Rev. B* **52**, 6796 (1995).

¹⁰Our treatment is in some respects similar to M. Fabrizio, *Phys. Rev. B* **48**, 15 838 (1993).

¹¹T. Giamarchi and H. Schulz, *Phys. Rev. B* **37**, 325 (1988).

¹²See, e.g., J. Solyom, *Adv. Phys.* **28**, 201 (1979).

¹³P. W. Anderson, *Science* **235**, 1196 (1987).

¹⁴C. M. Varma and A. Zawadowski, *Phys. Rev. B* **32**, 7399 (1985).

¹⁵L. Balents and M. P. A. Fisher (unpublished).

¹⁶T. Kimura *et al.*, *Phys. Rev. B* **49**, 16 852 (1994).

¹⁷A. W. W. Ludwig, in *Quantum Field Theory and Condensed Matter Physics: Proceedings of the Fourth Trieste Conference, Trieste, Italy, 1991*, edited by S. Randjbar-Daemi and Yu Lu (World Scientific, Singapore, 1994).

¹⁸S. A. Brazovskii and V. M. Yakovenko, *Sov. Phys. JETP* **62**, 1340 (1985); C. Bourbonnais and L. G. Caron, *Int. J. Mod. Phys. B* **5**, 1033 (1991); V. M. Yakovenko, *JETP Lett.* **56**, 510 (1992).

¹⁹K. Penc and J. Solyom, *Phys. Rev. B* **41**, 704 (1990).

²⁰H. Lin, L. Balents, and M. P. A. Fisher (unpublished).